Dispersion, diffraction and surface waves in semi-infinite metal-dielectric superlattices

Slobodan Vuković,[a] Carlos J. Zapata-Rodríguez,[b] Juan J. Miret,[c] and Zoran Jaksić[a]

[a]Center of Microelectronic Technologies and Single Crystals, Institute of Chemistry, Technology and Metallurgy, University of Belgrade, Njegoeva 12, 11000 Belgrade, Serbia;
[b]Department of Optics, University of Valencia, Dr. Moliner 50, 46100 Burjassot, Spain;
[c]Department of Optics, Pharmacology and Anatomy, University of Alicante, P.O. Box 99, Alicante, Spain

ABSTRACT

We investigate spatial-dispersion properties of hybrid surface waves propagating in the boundary of a semi-infinite layered metal-dielectric nanostructure. Electromagnetic fields can be dramatically affected by a nonlocal optical response of the plasmonic lattice. We demonstrate that the use of the so called effective medium approximation (EMA) is not justified if the thickness of a metallic layer becomes of the order of the metal skin depth. We compare the results obtained by means of EMA with computer solutions of Maxwell's equation, including losses in the metal.

Keywords: hybrid surface waves, superlattices, plasmonics

1. INTRODUCTION

Recently, metallodielectric superlattices are receiving more and more attention because of their extraordinary optical properties such as near-field focusing, subwavelength imaging, and negative refraction.[1–3] The inclusion of metallic elements is responsible for the excitation of plasmonic resonances on the surfaces of such an anisotropic metamaterial. Other kind of polariton surface waves may exists, for instance, fields propagating along the optical axis when the plasmonic crystal is cut normally to the orientation of the layers.[4] Interestingly, fundamental properties of these surface waves may be considered by using the effective-medium model.[5]

Here we demonstrate the existence of surface waves in the layered metamaterial with oblique propagation. These surface waves are not TM polarized but they have hybrid polarization. We investigate the spatial dispersion of these hybrid surface waves. We put emphasis in the case that the thickness of a metallic layer becomes comparable with the metal skin depth. Then, electromagnetic field properties in such a nanostructure can be dramatically affected by a nonlocal optical response and coupling of surface plasmon polaritons at different metal-dielectric interfaces.[6,7] We demonstrate that the use of the so called EMA, as a conventional approach for describing optical properties of the layered structures, and their description as uniaxial metamaterials (plasmonic crystals) is not justified, in general.

For simplicity, we first confine ourselves to the case that EMA is valid and, therefore, the superlattice behaves essentially like a uniaxial plasmonic crystal with the main optical axis perpendicular to the metal-dielectric interfaces. Then we may follow Dyakonov studies[8] in order to obtain an analytical expression for the spatial dispersion of these surface waves. Later we present numerical simulations that confirms the invalidity of EMA-Dyakonov approach for most practical cases. The propagation of surface modes obliquely to the optical axes occurs under favorable conditions regarding the thickness of the layered elements and the dielectric permittivity of the constituent materials. In opposition with pure Dyakonov waves, here we find solutions within a wide angular spectrum. Finally, losses in the metallic layers have great influence on the solutions of Maxwell's equations. However, we will demonstrate that dissipative effects are minimized when the *center of mass* of the surface wave shifts in direction to the isotropic transparent medium.

Metamaterials VII, edited by Allan D. Boardman, Nigel P. Johnson, Richard W. Ziolkowski, Proc. of SPIE
Vol. 8423, 84231W · © 2012 SPIE · CCC code: 0277-786X/12/$18 · doi: 10.1117/12.921885

Downloaded from SPIE Digital Library on 20 Jun 2012 to 147.156.26.41. Terms of Use: http://spiedl.org/terms

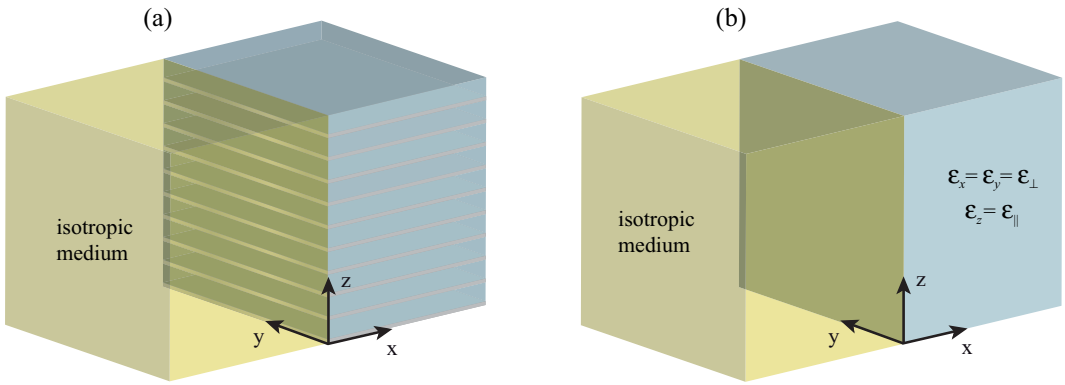

Figure 1. (a) Schematic setup under study consisting of a semi-infinite Ag-GaAs superlattice and a cover dielectric, either N-BAK1 or P-SF68 [SCHOTT]. (b) Graphical representation by using the effective-medium approach.

2. DYAKONOV-LIKE SURFACE WAVES

Let us first consider a bilayered superlattice made of two different materials that are alternatively stacked along the z-direction. The unit cell of the 1D photonic lattice consists of a transparent material of dielectric constant ϵ_d and slab width w_d followed by a metal of parameters ϵ_m and w_m, respectively. In our numerical simulations we set $\epsilon_d = 12.5$ and $\epsilon_m = -103.3 + i8.1$ at a wavelength $\lambda_0 = 1.55$ μm corresponding to GaAs and Ag, respectively. This metamaterial is located in the semi-space $x > 0$. Beside the periodic medium we place an isotropic material of dielectric constant ϵ, as shown in Fig. 1(a). On its boundary at the plane $x = 0$ we expect to find bound waves, and therefore the electromagnetic fields fall off exponentially when $|x| \to \infty$.

In order to obtain analytical solutions of Maxwell's equations corresponding to surface waves on the superlattice boundary, we configured the optical anisotropy of our periodic structure by employing average estimates. In particular, the form birefringence was modeled by the effective-medium theory.[9] The validity of this approximation is limited to periods $\Lambda = w_d + w_m$ that are much shorter than the wavelength, $\Lambda \ll \lambda_0$. In this case, the superlattice behaves like a uniaxial crystal whose optical axis is perpendicular to the interfaces, that is the z-axis. The EMA estimates the relative permittivity along the optical axis by

$$\frac{1}{\epsilon_{||}} = \frac{1-f}{\epsilon_d} + \frac{f}{\epsilon_m}, \tag{1}$$

and

$$\epsilon_\perp = (1-f)\,\epsilon_d + f\epsilon_m, \tag{2}$$

transversally, considering that the filling factor of the metal is $f = w_m/(w_d + w_m)$. In Fig. 1(b) we plot the complete picture as a result of being under the effective-medium model.

In Fig. 2 we represent the effective birefringence $\Delta n = \sqrt{\epsilon_{||}} - \sqrt{\epsilon_\perp}$ corresponding to the Ag-GaAs superlattice. For simplicity we have neglected material losses, thus setting $\mathrm{Im}(\epsilon_m) = 0$. In our case, even a small filling factor of the metallic composite leads to an enormous birefringence. The term $\Delta\epsilon = \epsilon_{||} - \epsilon_\perp$ has approximately a linear variation upon f, unlike Δn, up to $f_{\max} = 0.108$ where $\epsilon_\perp = 0$, as shown in the inset of Fig. 2. A filling factor higher than $f_{\max}$ provides negative values of $\epsilon_\perp$, associated with hyperbolic dispersion.[10] If $f \ll 1$ we observe that

$$\Delta\epsilon = \frac{(\epsilon_d + \epsilon_m)^2}{-\epsilon_m} f. \tag{3}$$

Since $\epsilon_m < 0$ therefore $\Delta\epsilon > 0$ (and $\Delta n > 0$), that is, birefringence is positive. Despite $f_{\max} \ll 1$, the maximum birefringence achievable reaches $[\Delta n]_{\max} = 3.77$. Note that $\Delta n = 0.0084$ for crystalline quartz, and $\Delta n = 0.22$

Further author information: (Send correspondence to C.J.Z.R.)
C.J.Z.R.: E-mail: carlos.zapata@uv.es, Telephone: +34 96 354 38 05

Downloaded from SPIE Digital Library on 20 Jun 2012 to 147.156.26.41. Terms of Use: http://spiedl.org/terms

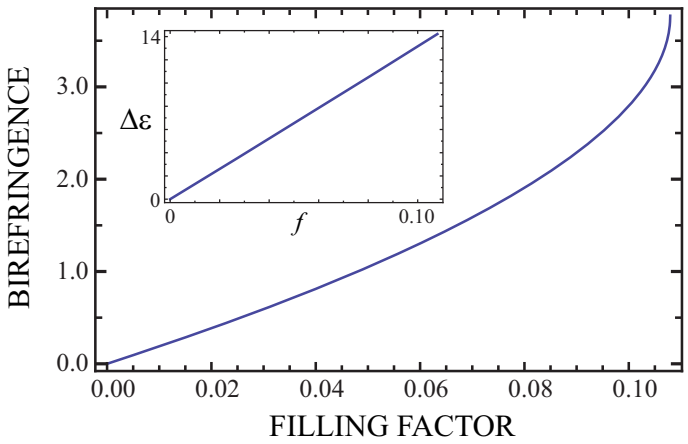

Figure 2. Form birefringence Δn of the 1D multilayered Ag-GaAs structure in terms of the metallic filling factor, f. The inset shows changes of $\Delta\epsilon = \epsilon_{||} - \epsilon_{\perp}$ for the same range of filling factors.

for liquid crystal BDH-E7,[11] implying that birefringence in our artificial uniaxial crystal is greater by more than one order of magnitude.

Once the superlattice may be treated like an anisotropic media, we may determine the analytical diffraction equation giving the 2D wave vector of hybrid surface waves propagating at $x = 0$. In the isotropic media we consider homogeneous TE and TM waves with real components k_y and k_z of the wave vector. Note that these wave fields are inhomogeneous along the x-axis in a direct proportion to $\exp(-\kappa|x|)$, where

$$\kappa = \sqrt{k_y^2 + k_z^2 - k_0^2\epsilon}. \tag{4}$$

and $k_0 = 2\pi/\lambda_0$. On the other side of the boundary, the ordinary and extraordinary waves in the *effective* uniaxial medium follow also exponential decays with rates given by

$$\kappa_o = \sqrt{k_y^2 + k_z^2 - k_0^2\epsilon_{\perp}}, \text{ and} \tag{5}$$

$$\kappa_e = \sqrt{k_y^2 + k_z^2\epsilon_{||}/\epsilon_{\perp} - k_0^2\epsilon_{||}}, \tag{6}$$

respectively. To derive the Dyakonov equation providing a map of allowed (k_y, k_z) we finally consider that the transverse components of the electric field and the magnetic field are continuous at $x = 0$. The resulting diffraction equation is[8]

$$(\kappa + \kappa_e)(\kappa + \kappa_o)(\epsilon\kappa_o + \epsilon_{\perp}\kappa_e) = \left(\epsilon_{||} - \epsilon\right)(\epsilon - \epsilon_{\perp})\, k_0^2\kappa_o. \tag{7}$$

By meticulous inspection of Eq. (7), and assuming that all dielectric constants and decay rates involved are positive, we find that

$$\epsilon_{\perp} < \epsilon < \epsilon_{||}, \tag{8}$$

which is necessary for the surface waves to exist. As a consequence, we require that the anisotropic medium exhibits a positive birefringence.

Figures 3(a)-(b) depict the solutions of Eq. (7) for two different anisotropic media. In all cases, the wavelength is set $\lambda_0 = 1.55$ μm, and the isotropic cover is N-BAK1 with dielectric constant $\epsilon = 2.42$. In (a) we evaluate Eq. (7) for a liquid crystal E7 using $\epsilon_{||} = 2.98$ and $\epsilon_{\perp} = 2.31$. In this case Dyakonov waves propagate in a narrow angular domain $\Delta\theta = \theta_{\max} - \theta_{\min}$, where θ stands for the angle of the 2D vector (k_y, k_z) with respect to the optical axis, that is, $\tan\theta = k_y/k_z$. For the liquid crystal E7 we estimate $\Delta\theta = 0.92°$ around a mean angle $\bar{\theta} = 26.6°$. Note that $\Delta\theta$ is extremely high if it is compared with the angular range obtained for optical crystals like quartz exhibiting a standard birefringence. In order to increase even more the angular range $\Delta\theta$ we consider in (b) a plasmonic crystal made of Ag-GaAs. For a filling factor $f = 0.10$, the silver composite provides

Downloaded from SPIE Digital Library on 20 Jun 2012 to 147.156.26.41. Terms of Use: http://spiedl.org/terms

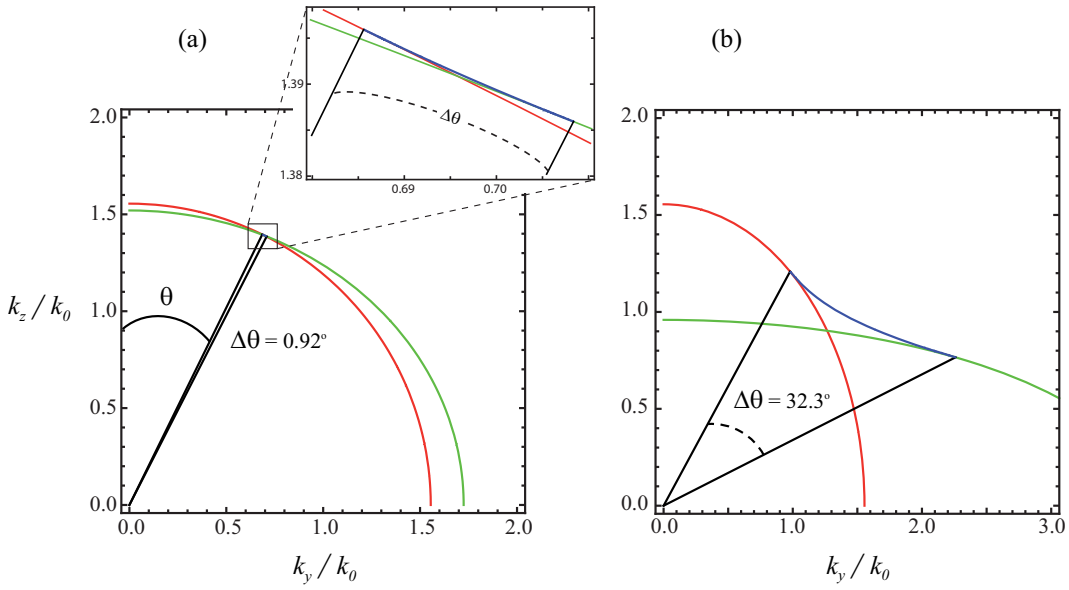

Figure 3. Solutions of the Dyakonov equation (7) for (a) an anisotropic E7 liquid crystal, and (b) the Ag-GaAs superlattice of $f = 0.10$ depicted in Fig. 1. The cover is N-BAK1, a solid transparent material of refractive index $n = 1.56$.

$\epsilon_{||} = 14.08$ and $\epsilon_{\perp} = 0.92$, thus birefringence gives $\Delta n = 2.79$. Eq. (7) provides solutions for angles ranging from $\theta_{\min} = 39.0°$ up to $\theta_{\max} = 71.3°$. As a consequence the angular range $\Delta\theta = 32.3°$ has increased by more than one order of magnitude.

3. EXACT SOLUTIONS OF MAXWELL'S EQUATIONS

The EMA is limited to a width of the metallic slabs that is much lower than the wavelength, $w_m \ll \lambda_0$. However, this condition must be taken into account with care since the skin depth of noble metals is extremely small, $\lambda_s \approx c/\omega_p$, where ω_p is the plasma frequency of the metal. In the case of silver we estimate that $\lambda_s = 24$ nm. If the width of the metallic layers comes close to the skin depth, nonlocal effects cause that the EMA considerably deviates from exact calculations.[12] Moreover, in practical terms, experimental realizations of multilayered devices rarely go to widths below 10 nm. As a consequence, it is highly appropriate to estimate discrepancies derived by these nonlocal effects.

Next we evaluate the full-wave solutions of Maxwell's equations leading to the spatial spectrum of Bloch waves that propagate in the metal-dielectric lattice. In this case k_z represents the pseudo-moment of Bloch waves. In Fig. 4 we show the spatial dispersion equation[9]

$$\cos(k_z \Lambda) = \cos(k_{mz} w_m) \cos(k_{dz} w_d) - \eta_{o,e} \sin(k_{mz} w_m) \sin(k_{dz} w_d), \tag{9}$$

corresponding to S-polarized (ordinary) and P-polarized (extraordinary) waves propagating within the periodic Ag-GaAs structure with $f = 0.10$. Note that

$$\eta_o = \frac{1}{2}\left(\frac{k_{dz}}{k_{mz}} + \frac{k_{mz}}{k_{dz}}\right), \text{ and} \tag{10}$$

$$\eta_e = \frac{1}{2}\left(\frac{\epsilon_m k_{dz}}{\epsilon_d k_{mz}} + \frac{\epsilon_d k_{mz}}{\epsilon_m k_{dz}}\right), \tag{11}$$

are coefficients applied in Eq. (9) for ordinary and extraordinary waves, respectively. Finally

$$k_t^2 + k_{qz}^2 = \epsilon_q k_0^2, \tag{12}$$

Downloaded from SPIE Digital Library on 20 Jun 2012 to 147.156.26.41. Terms of Use: http://spiedl.org/terms

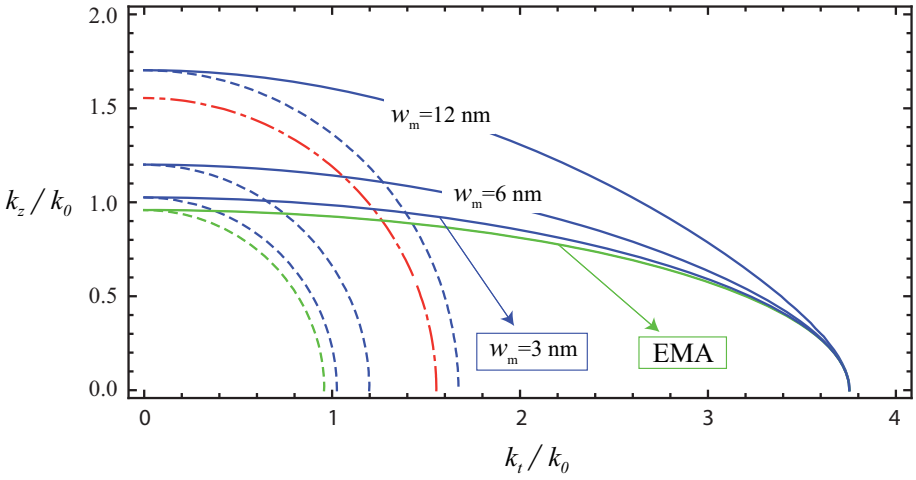

Figure 4. Isofrequency curves evaluated from Eq. (9) for a Ag-GaAs superlattice with filling factor $f = 0.10$. Results for TM (solid lines) and TE waves (dashed lines) for different values of w_m. The dotted-dashed line corresponds to the isofrequency curve for the isotropic N-BAK1 cover. Note that losses in silver are not considered here.

being $k_t^2 = k_x^2 + k_y^2$, which represents the dispersion equation for bulk waves within GaAs ($q = d$) and silver ($q = m$).

For clarity, the numerical simulations ignore absorption in silver. In Fig. 4 we observe that the EMA is accurate for $w_m = 3$ nm. However, deviations of the dispersion contour are evident for higher widths. Apparently Eq. (9) provides appropriate solutions in the vicinity of $k_z = 0$ for TM waves. On the opposite side, propagation along the z-axis, where $k_x = k_y = 0$, presents the highest discrepancies. This is caused by the most significant contribution of the skin depth in diffraction. As a result, the pseudo-moment k_z increases for higher w_m, an effect that is observed simultaneously for TM and TE waves. For TE polarization, isotropy of the isofrequency curve is practically conserved, but effective $\epsilon_\perp$ increases for higher w_m, e.g., $n_\perp = 1.70$ and $n_{||} = 1.67$ for $w_m = 12$ nm. Thus form birefringence is reduced in the plasmonic crystal.

Anisotropy drop caused by the small skin depth has a great impact on the excitation of Dyakonov-like surface waves. Increasing $\epsilon_\perp$ and simultaneously keeping $\epsilon_{||}$ leads to a significant modification of the isofrequency curve derived from Eq. (7). Moreover, we may get to the point that the photonic device cannot sustain surface waves if the value of $\epsilon_\perp$ exceeds that of ϵ. To avoid this drawback, we may use a cover of higher refractive index.

Heretofore we have eluded another important matter in plasmonic devices in relation with dissipative effects in metallic elements. In order to tackle this problem, we numerically evaluate the pseudo-moment k_z for given real values of k_y. Since $\mathrm{Im}\,(\epsilon_m) \neq 0$ then k_z becomes complex. This means that the surface wave cannot propagate indefinitely and there exists an energy attenuation length given by $l = (2\mathrm{Im}[k_z])^{-1}$. On the other hand, it is necessary to impose that the real part of the parameters κ, κ_o and κ_e given in Eqs. (4)-(6) are all positive. Note that $\epsilon_\perp$ and $\epsilon_{||}$ are also complex. This fact leads to effective field decays for $|x| \to \infty$ and, therefore, confinement near the plane surface $x = 0$.

Fig. 5(a) represents the spatial dispersion of Dyakonov-like solutions in the plane $k_y\mathrm{Re}(k_z)$. We also plot the isofrequency curves for Bloch modes shown in Fig. 4, provided $k_x = 0$, corresponding to a metallic composite of $f = 0.10$ and $w_m = 12$ nm. The numerical simulations are performed using a commercial software (COMSOL Multiphysics) based on the finite-element method (FEM). From our computer simulations we have not observed surface waves for a cover of N-BAK1, where $n = 1.56$. This case is not consistent with Eq. (8) since $n_\perp = 1.70$ and $n_{||} = 3.75$. Fig. 5(a) depicts the spatial dispersion when $n = 1.95$ corresponding to P-SF68 [SCHOTT]. The boundaries of such curve are established according to the ability of the electromagnetic field to be confined in the neighborhood of $x = 0$, which leads to a certain degree of inaccuracy from computational grounds. In Fig. 5(b) we plot $\mathrm{Im}(k_z)/\mathrm{Re}(k_z)$ in the range of existence of the surface waves. For paraxial surface waves with low k_y, we observe that $\mathrm{Im}(k_z) \ll \mathrm{Re}(k_z)$. This is caused by a large shift of the intensity maximum toward the

Downloaded from SPIE Digital Library on 20 Jun 2012 to 147.156.26.41. Terms of Use: http://spiedl.org/terms

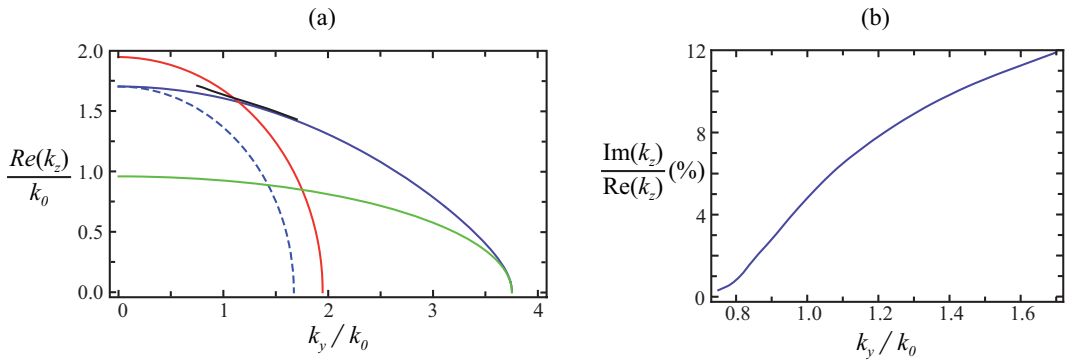

Figure 5. (a) Isofrequency curve corresponding to hybrid surface waves existing at the boundary between a semi-infinite P-SF68 cover and a plasmonic Ag-GaAs superlattice of $f = 0.10$ and $w_m = 12$ nm. In (b) we represent the imaginary part of k_z obtained from our FEM simulations.

transparent isotropic medium. In this case $\mathrm{Re}(\kappa) \ll \mathrm{Im}(\kappa)$. On the other hand, nonparaxial waves with high k_y are characterized by deep energy penetration inside the plasmonic superlattice. As a consequence, losses in the metal are manifested by rising significantly the values of $\mathrm{Im}(k_z)$.

4. CONCLUSIONS

We conclude that oblique surface waves may propagate at the boundary between a plasmonic bilayer superlattice and an isotropic transparent material. These modes are not TM-polarized, since all three spatial components of the electric, as well as of the magnetic field are involved. That is, these modes are hybrid. Realistic slab widths lead to solutions that deviate significantly from the results of EMA and Dyakonov analysis. Our FEM simulations prescribe the use of cover materials of a higher refractive index for the existence of surfaces waves. A wide angular range of surface waves is reachable with large to moderate energy attenuation lengths. We remark that the properties of the resulting bound states change rapidly with the refractive index of the surrounding medium (cover), which suggests potential applications for chemical and biological sensors.

ACKNOWLEDGMENTS

This research was funded by the Spanish Ministry of Economy and Competitiveness under the project TEC2009-11635, by the Qatar National Research Fund under the project NPRP 09-462-1-074, and by the Serbian Ministry of Education and Science under the projects III 45016 and TR 32008.

REFERENCES

1. M. Scalora, M. J. Bloemer, A. S. Pethel, J. P. Dowling, C. M. Bowden, and A. S. Manka, "Transparent, metallo-dielectric, one-dimensional, photonic band-gap structures," *J. Appl. Phys.* **83**, pp. 2377–2383, 1998.
2. P. A. Belov and Y. Hao, "Subwavelength imaging at optical frequencies using a transmission device formed by a periodic layered metal-dielectric structure operating in the canalization regime," *Phys. Rev. B* **73**, p. 113110, 2006.
3. A. Pastuszczak and R. Kotyński, "Optimized low-loss multilayers for imaging with sub-wavelength resolution in the visible wavelength range," *J. Appl. Phys.* **109**, p. 084302, 2011.
4. S. M. Vukovic, I. V. Shadrivov, and Y. S. Kivshar, "Surface Bloch waves in metamaterial and metal-dielectric superlattices," *Appl. Phys. Lett* **95**, p. 041902, 2009.
5. S. M. Rytov, "Electromagnetic properties of layered media," *Sov. Phys. JETP* **2**, p. 466, 1956.
6. S. M. Vuković, J. J. Miret, C. J. Zapata-Rodríguez, and Z. Jakšić, "Oblique surface waves at an interface of metal-dielectric superlattice and isotropic dielectric," *Phys. Scripta* , in print.
7. J. J. Miret, C. J. Zapata-Rodríguez, Z. Jakšić, S. M. Vuković, and M. R. Belić, "Hybrid surface waves in semi-infinite metal-dielectric lattices," *Opt. Lett.* , submitted.

Downloaded from SPIE Digital Library on 20 Jun 2012 to 147.156.26.41. Terms of Use: http://spiedl.org/terms

8. M. I. D'yakonov, "New type of electromagnetic wave propagating at an interface," *Sov. Phys. JETP* **67**, pp. 714–716, 1988.
9. P. Yeh, *Optical Waves in Layered Media*, Wiley, New York, 1988.
10. B. Wood, J. B. Pendry, and D. P. Tsai, "Directed subwavelength imaging using a layered metal-dielectric system," *Phys. Rev. B* **74**, p. 115116, 2006.
11. S.-T. Wu, U. Efron, and L. D. Hess, "Birefringence measurements of liquid crystals," *Appl. Opt.* **23**, pp. 3911–3915, 1984.
12. J. Elser, V. A. Podolskiy, I. Salakhutdinov, and I. Avrutsky, "Nonlocal effects in effective-medium response of nanolayered metamaterials," *Appl. Phys. Lett.* **90**, p. 191109, 2007.

Downloaded from SPIE Digital Library on 20 Jun 2012 to 147.156.26.41. Terms of Use: http://spiedl.org/terms